Chapter 8

IRRADIATION EFFECTS ON COMPATIBILITY OF STRUCTURAL MATERIALS WITH LEAD-BISMUTH EUTECTIC (LBE)*

8.1 Introduction

The interaction between several materials in the presence of static or flowing lead alloys was performed in a number of laboratories at different temperatures, flow rates, oxygen contents, surface and heat treatment conditions. In the past few years many results concerning corrosion attack and possibilities to prohibit it were generated in the 5th FP (TECLA) [JNM, 2004] and some investigations are still ongoing in the 6th FP (DEMETRA) [Fazio, 2005]. The examinations are in the early stage concerning mechanical tests in the presence of lead or lead alloy and may have an influence on mechanical properties. As of this date there are no other sources of data available and the chapter can only focuses on a very few sets of data. Of great interest is to understand the mechanism of liquid metal embrittlement (LME) and to identify the cause of damage. In Chapters 6 and 7 of this handbook the compatibility of structural materials with LBE and mechanical properties in LBE are covered. In Chapter 9 the knowledge is summarised on lead and LBE corrosion protection existing up to now.

Another important issue is the material behaviour during irradiation. The change of material properties because of irradiated with protons and/or neutrons has to be fully understood. The effects of irradiation on mechanical properties generally manifest themselves on one hand as an increase in the yield stress (radiation hardening) and on the other hand as a decrease in ductility (radiation embrittlement) [Jung, 2002].

The main objective therefore is to determine whether irradiation will promote embrittlement and corrosion attack by liquid metal. The investigations are just in the early stage and only a limited number of experiments have been launched in this field up to now.

In the experimental facility LiSoR at PSI the specimens are placed directly in the LBE flow while irradiated with protons/neutrons. The experimental conditions for operating the loop and the irradiation beam parameters are presented and the results of analysis of the irradiated specimens (surface and cross-section) and of the tensile tests are discussed in Section 8.2. Pre-oxidised martensitic ferritic steel HT9 has been irradiated with protons at the LANSCE WNR facility in Los Alamos, USA, in the presence of LBE. The results are discussed in Section 8.2 as well.

SCK•CEN has irradiated the steels AISI 316L, T91, EM10 and HT9 in the BR2 reactor in Mol, Belgium. After irradiation, tensile tests were performed in the presence of LBE. The experimental conditions and the results are presented in Section 8.3.

At PSI several different materials (in contact with Pb and LBE) have been irradiated in the SINQ facility with protons/neutrons. Mechanical tests are foreseen to be performed in LBE. Some details concerning the test programmes including the irradiation conditions are described in Section 8.4.

---

* *Chapter lead: Heike Glasbrenner (PSI, Switzerland). For additional contributors, please see the List of Contributors at the end of this work.*

In Section 8.5 a brief overview on the irradiation experiments planned to be performed within the DEMETRA (6^{th} FP) is given.

8.2 Irradiation of ferritic-martensitic steel T91 with protons and neutrons in LBE (PSI)

The DIN 1.4903 steel 9Cr1MoVNb named T91 was supplied by the company CLI-FAFER (France) and has a composition in wt.% of 8.41 Cr, 0.08 Ni, 0.95 Mo, 0.44 Mn, 0.31 Si, 0.1 C, 0.25 V, 0.08 Nb, 0.24 Si, 0.035 Cu, 0.002 S with Fe in balance. The material was delivered in standard heat treated conditions, i.e. the steel was normalised at 1070°C for 1 h followed by air cooling, and then tempered at 765°C for 1 h followed by air cooling.

8.2.1 LiSoR

LiSoR (Liquid-metal/Solid-metal Reaction) is a unique facility to investigate simultaneously the influence of flowing LBE, static mechanical stress and additional fluctuating thermal stress under irradiation of a steel probe. LiSoR facility is actually a LBE loop installed at a proton beam line of Injector-I at PSI. The energy of the proton beam is 72 MeV. Protons with this energy can penetrate about 10 cm in steels or LBE [Kirchner, 2003].

8.2.2 Irradiation

For performing the post-irradiation experiments (PIE) the samples of interest are the test-section tube (TS-tube) and inner tensile-stressed specimen (TS-specimen) in the test section. Both the wall of the TS-tube and the TS-specimen are 1 mm in thickness. Figure 8.2.1 describes the geometry of the specimen. In Figure 8.2.2 the sketches show the test tube made of T91 and the cross-section including the specimen and the flowing LBE.

During irradiation (including beam-off time) a constant mechanical load was applied upon the tensile specimen and the temperature of inlet LBE was constantly controlled at 300°C. In the TS-tube and TS-specimen the irradiation areas are about 5.5×14 mm^2. In the irradiation areas the proton beam induced localised temperature increase and thermal stress oscillated with the wobbled proton beam at a frequency of about 2 Hz. The materials and irradiation parameters are listed in Table 8.2.1 for the four irradiation campaigns, LiSoR-2 to LiSoR-5. The details of the experiments and the temperature and stress distributions are given in [Glasbrenner, 2005a], [Kirchner, 2003], [Samec, 2005]. As an example Figure 8.2.3 shows the calculated temperature, stresses in longitudinal/transversal directions and shear stress changing with time at a point in the irradiation area of the TS-specimen LiSoR-5 [Samec, 2005].

Figure 8.2.1. Nominal dimensions of the specimen irradiated in test section no. 2 to 5

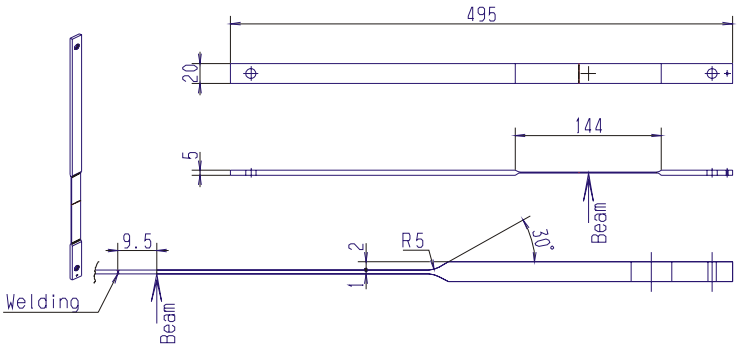

Figure 8.2.2. Sketches show the test tube and its cross-section including the specimen and flowing LBE

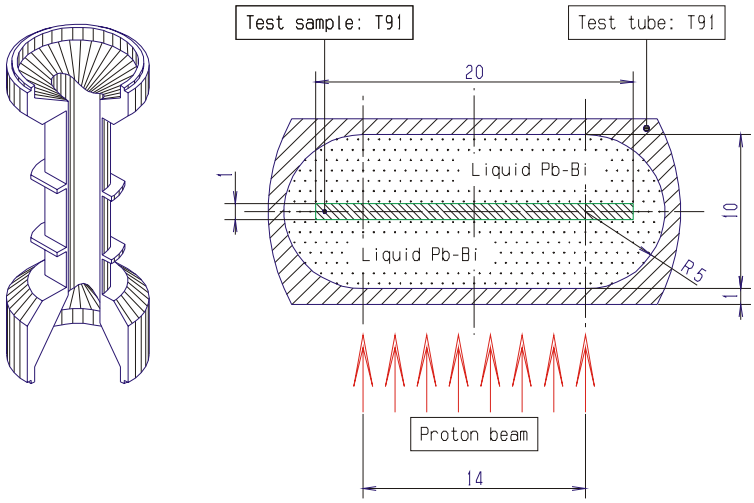

Table 8.2.1. Materials and irradiation conditions of the TS-tubes and TS-specimens of LiSoR-2 to LiSoR-5

		LiSoR-2	LiSoR-3	LiSoR-4	LiSoR-5
Irradiation time		34 h	264 h	144 h	724 h
Material	TS-tube TS-specimen	T91-A[1] T91-B[2]	T91-A* T91-B*	T91-A* T91-B*	T91-A* T91-C[3]
Averaged proton energy [4]	TS-tube TS-specimen	70 MeV 40 MeV	70 MeV 40 MeV	70 MeV 40 MeV	70 MeV 40 MeV
Beam current		50 μA	15 μA	30 μA	30 μA
Peak oscillating temp. LBE-surf. [5]	TS-tube TS-specimen	650°C 580°C	330°C 324°C	400°C 380°C	400°C 380°C
Peak oscillating. temp. maximum [6]	TS-tube TS-specimen	– –	380°C 345°C	550°C 440°C	550°C 440°C
Maximum stress[7]	TS-tube TS-specimen	– 200 MPa	25 MPa 200 MPa	75 MPa 200 MPaC	75 MPa 200 MPa
Irradiation dose [8]	TS-tube TS-specimen	0.1 0.075	0.2 0.15	0.2 0.15	1.0 0.75
He concentration [9]	TS-tube TS-specimen	3.6 appm 2.6 appm	7.2 appm 5.2 appm	7.2 appm 5.2 appm	36 appm 26 appm

[1] T91-A, the material of the tube produced by Creusot Loire Industrie (France) and has a composition in wt.% of 8.26 Cr, 0.13 Ni, 0.95 Mo, 0.43 Si, 0.38 Mn, 0.1 C, 0.2 V, 0.017 P, 0.065 Nb and with Fe in balance.

[2] T91-B, the material of the TS-specimen: from SPIRE programme supplied by Ugine (France) and has a composition in wt.% of 8.63 Cr, 0.23 Ni, 0.95 Mo, 0.31 Si, 0.43 Mn, 0.1 C, 0.21 V, 0.02 P, 0.09 Nb and with Fe as balance. The material was normalised at 1040°C for 1 h followed by air cooling, and then tempered at 760°C for 1 h followed by air cooling.

[3] T91-C, the material of the TS-specimen of LiSoR-5.

[4] [Kirchner, 2003] Figure 8.

[5] [Samec, 2005].

[6] [Samec, 2005]. The maximum temperature in the TS-specimen is in the central position (0.5 mm depth) while for the tube it is at the outer surface.

[7] [Samec, 2005]. For the TS-tube it is the maximum shear stress. In fact the TS-tube has a maximum compression stress which is 6 times larger than the shear stress.

[8] [Samec, 2005].

[9] The helium concentration of LiSoR-2 was measured [Dai, 2006b]. The others were calculated using LiSoR-2 data.

Figure 8.2.3. The time dependence of temperature, stresses in longitudinal/transversal directions and shear stress at a point in the irradiation area of the TS-specimen LiSoR-5 calculated with the ANSYS code [Samec, 2005]

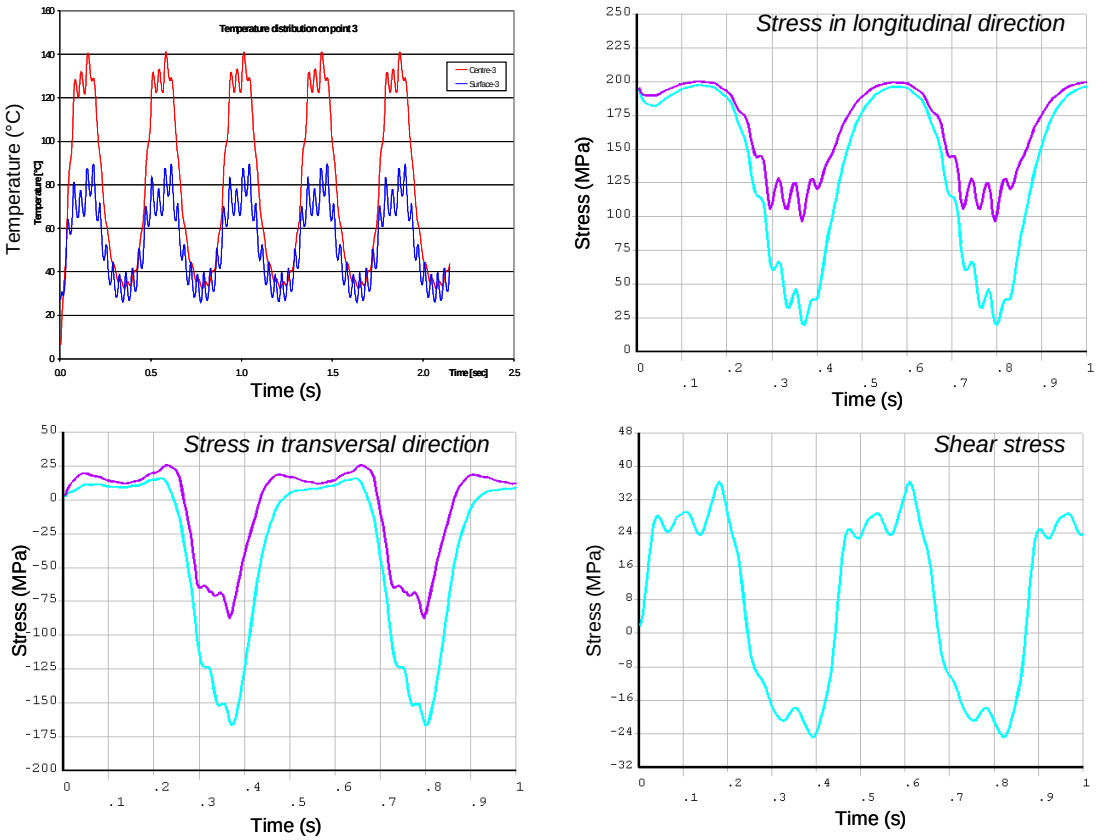

8.2.3 Surface analyses

The surface analyses of LiSoR samples have been performed in different ways: visual inspection (photography), SEM, EPMA and SIMS.

The photos of the visual inspection have been taken from the irradiation areas of both the TS-tubes and the TS-specimens of the four irradiations, as shown in Figure 8.2.4. In the upper photos the beam foot print on each TS-tube can be clearly seen. In the LiSoR-2 TS-tube, a crack was formed due to high temperature and high thermal stress induced by small beam size [Dai, 2004]. No other evident damages were observed in other TS-tubes. The LBE on LiSoR-2 TS-tube was leaking out from the crack. On the surfaces of the TS-specimens one can see some remaining of LBE. On the TS-specimens of LiSoR-2 and -5 a significant amount of adherent LBE is visible, which can be attributed to either higher temperature (LiSoR-2) or longer time of exposure (LiSoR-5) compared to LiSoR-3 and -4. The irradiation areas in LiSoR-2 and -5 specimens are quite easy to recognise, while in those of LiSoR-3 and -4 are more difficult. There are some deposits on the surfaces of LiSoR-2 and -5 specimens below the irradiation areas.

After the visual inspection, the TS-tubes and TS-specimens were cut with an EDM machine into small dog-bone shaped tensile samples for tensile testing, and the remaining pieces between the tensile samples were saved for TEM, SEM, SIMS, etc. analyses.

Figure 8.2.4. Upper photos show the TS-tubes of LiSoR-2 to -5 after irradiation. Lower photos show the TS-specimens of LiSoR-2 to -5 after irradiation. The arrows indicate the irradiation areas. The LBE flow direction is always upwards.

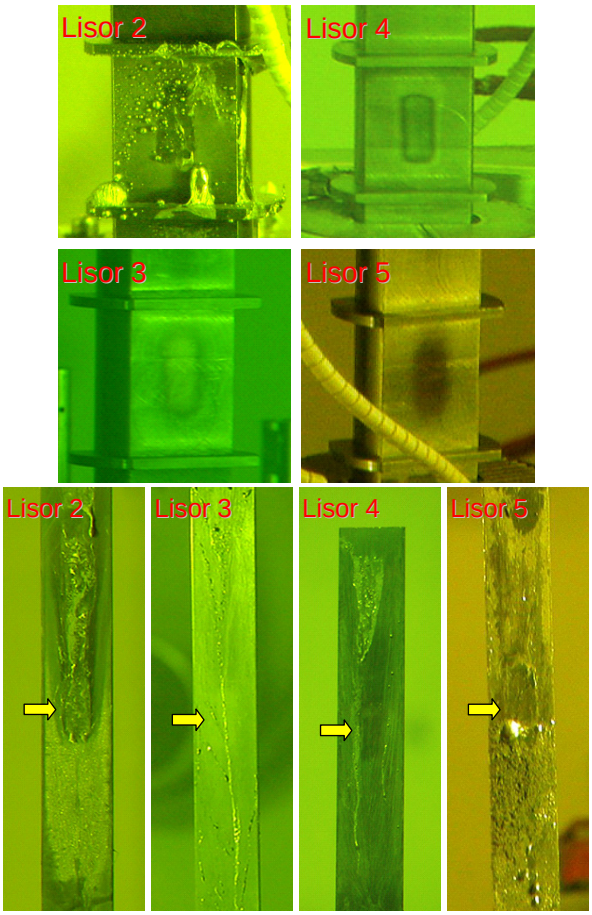

SEM (for low activity samples) or EPMA (for high activity samples) analyses were carried out to inspect the surface after irradiation in contact with LBE. As of this date samples from LiSoR-2, -3 and -5 have been analysed [Dai, 2004], [Glasbrenner, 2005a, 2005b, 2006].

The general feature is the formation of an oxide scale of up to few microns thickness on the surface in the irradiated areas, as illustrated in Figure 8.2.5. One can see that the oxide layer of LiSoR-2 is the thickest while that of LiSoR-3 is thinnest. From the irradiation conditions given in Table 8.2.1 one can conclude that the variation of the thickness of the oxide scale depends mainly on the irradiation temperature but that the irradiation time plays a role as well. However, this cannot be clarified here since the temperatures in the cases are different. This can be done when LiSoR-4 is inspected, since the temperatures of LiSoR-4 and LiSoR-5 are the same due to the identical irradiation parameters. From the difference between LiSoR-2 and the others, it is clear that the temperature effect is much more pronounced than the time effect.

The inner surface of the LiSoR-2 TS-tubes was not reworked after EDM wire cutting and before irradiation. After the leakage incident of LiSoR-2, the TS-tubes for the following LiSoR irradiations were polished on the inner surfaces to remove the micro-cracked layer. The three micrographs in Figure 8.2.6 show the inner surface of the LiSoR-2 TS-tube, the cross-sections of LiSoR-2 and LiSoR-3 TS-tubes, respectively. It can be seen that the surface after EDM cutting is very rough

(micrograph a) and cracks of a depth of about 10 μm were introduced in the surface layer (micrograph b). Mechanical polishing removed the damaged layer with microcracks of the inner surface layers of the LiSoR-3 to -5 TS-tubes (micrograph c).

The LBE on the surfaces of the TS-specimens of LiSoR-2 and LiSoR-5 have been analysed. Figure 8.2.5 shows an example of LiSoR-5. The region observed is below the irradiation area where a lot of precipitation adhered on the surface. The element analysis indicates Pb and Bi mostly separated due to re-crystallisation.

An important point should be noted is that, except for the TS-tube of LiSoR-2, no other microcracks were observed either in the TS-specimens or in the TS-tubes, even in the LiSoR-2 TS-specimen where the material of the irradiation area experienced about 120000 cycles of fatigue deformation at a relatively high stress and temperature [Glasbrenner, 2005a].

Figure 8.2.5. SEM (a and b) and EPMA (c) micrographs showing the cross-sections in the irradiation areas of (a) LiSoR-2, (b) LiSoR-3 and (c) LiSoR-5 TS-specimens

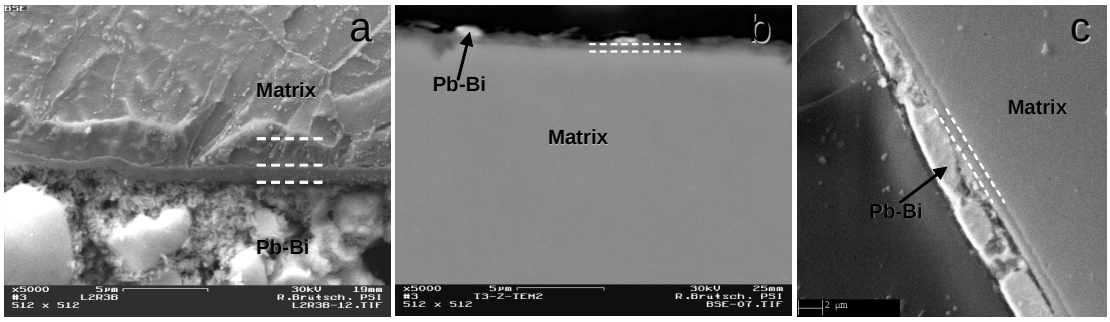

Figure 8.2.6. Graphs show (a) the inner surface of LiSoR-2 TS-tube, (b) the cross-sections of LiSoR-2 TS-tube and (c) the cross-sections of LiSoR-3 TS-tube

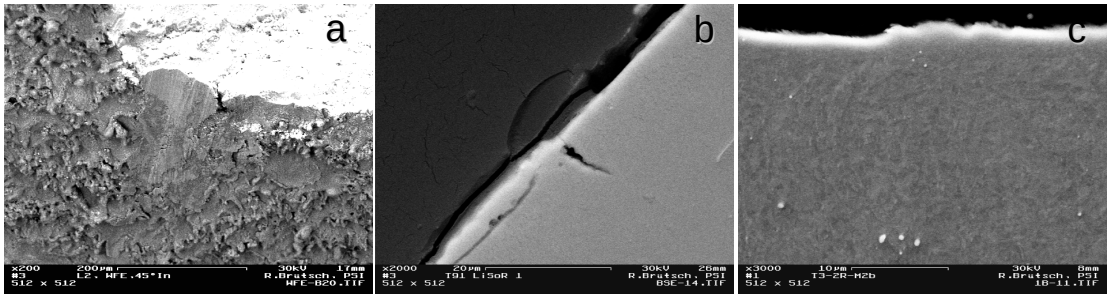

Figure 8.2.7. Wave Dispersive Spectrometers (WDS) analysis of LBE on the surface of the TS-specimen of LiSoR-5

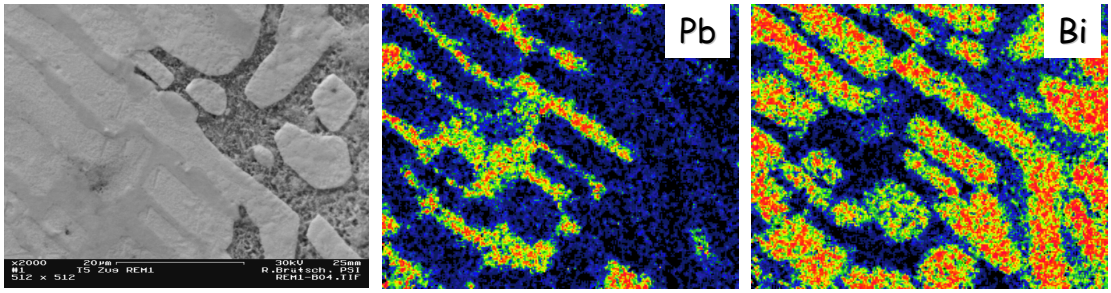

SIMS analyses were carried out on several samples of LiSoR-2 to -5. An element depth profile obtained on a sample from the irradiation area of the TS-specimen of LiSoR-3 is shown in Figure 8.2.8 [Glasbrenner, 2006].

Figure 8.2.8. Fe, Cr, FeO and Pb depth distribution profile measured in the irradiation area in LiSoR-3 TS-specimen

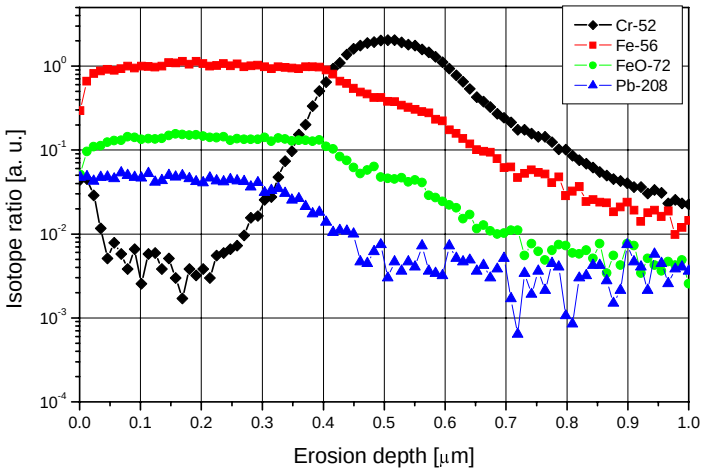

A small amount of ^{208}Pb was evident in the most outer layers of the sample, whereas the element Bi was not detected. The species ^{72}(FeO) and ^{56}Fe followed the same trend: Their amount stayed constant up to a depth of app. 400 nm, whereas ^{52}Cr was not detected in this area. With increasing depth a decrease of Fe and FeO took place and in parallel the amount of Cr increased from nearly zero, ran through a maximum and then decreased again. The maximum was in a depth of about 500 nm. The gradients of the Cr, Fe and FeO species achieved on the samples adjacent to the beam centre showed the same trend. In Figure 8.2.9 the Fe and Cr curves of the three samples from the TS-specimen of LiSoR-5 are put together in a graph for comparison. The thickness of the outer layer, constant amount of Fe and FeO without any Cr, is ~300 nm in a distance of 13 mm of the beam centre and ~250 nm in a distance of 24 mm. The peaks of Cr are ~ 400 nm at 13 mm distance and ~350 nm at 24 mm distance, respectively. It is well known that oxides formed on ferritic-martensitic steels consist of double structured oxides: the outer layer is the Cr-free iron oxide, and the layer beneath is a $FeCr_2O_4$ spinel. The present SIMS results agree with the general observations.

Figure 8.2.9. Fe (left) and Cr (right) depth distributions measured at different positions in LiSoR-3 TS-specimen

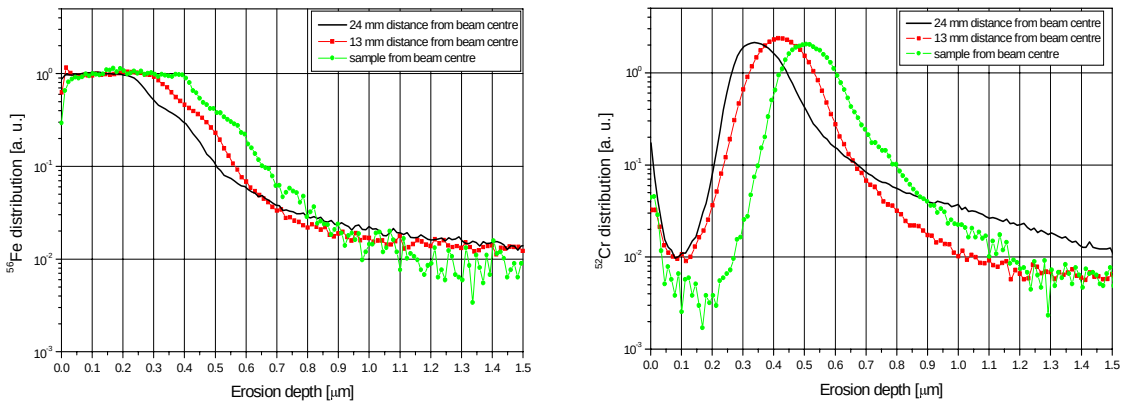

8.2.4 Tensile tests

As mentioned above, one of the main purposes of LiSoR experiments is to investigate the LBE embrittlement effects on T91 steel under irradiation. All the inner TS-specimens from LiSoR-2 to -5 were not broken during irradiation, although a mechanical loading of 200 MPa was always applied. This is at least a good indication that shows the material can withstand such mechanical load to a radiation damage level of about 0.75 dpa. To analyse the actual degradation of mechanical properties induced by LBE and irradiation, tensile tests were performed. The samples were divided into two groups. The first group included a part of samples from LiSoR-2 TS-specimens and all samples from the TS-tubes and TS-specimens of LiSoR-3 and LiSoR-5. They were tested in Ar (+2%H_2) atmosphere. The results of these tests should represent the original status of the T91 steel after irradiation in LiSoR. The second group included the rest of LiSoR-2 samples and the samples from LiSoR-4 which has almost the same irradiation dose as LiSoR-3. These samples were tested in LBE. These tests were intended to show additional effects from the testing environment in LBE. All the tests were performed at 300°C. The oxygen content in the LBE was less than 1 wppm [Dai, 2006c].

Figure 8.2.10 presents the tensile results of some LiSoR-3 and LiSoR-5 samples tested in Ar. The samples from the irradiation area of the TS-specimens demonstrate slight hardening induced by irradiation as expected (a and c). However, the hardening in the samples from the irradiation area of the TS-tubes is much less (b and d). This is due to the fact that the temperature in the irradiation area of the TS-tubes was higher ≥350°C, where irradiation hardening effects in martensitic steels are not significant. The ductility is only slightly reduced in samples of LiSoR-3, and more strongly in LiSoR-5. It is clear that the strong reduction of the ductility in LiSoR-5 samples is mostly due to the embrittlement of LBE. As can be seen in Figure 8.2.4, some LBE adhered on the surface of the TS-specimen of LiSoR-5. During EDM cutting or testing, the LBE could enter the microcracks on the side surfaces of the samples, which were produced by EDM cutting, and finally induced the embrittlement effect. For LiSoR-3 samples, since very little LBE adhered on the TS-specimen and TS-tube surfaces, the effect was not pronounced. On the other hand, the irradiation should have a synergetic effect. One can see that the embrittlement is more serious at higher doses in each individual case (a to d). Unfortunately, the present results are compromised by the effects the microcracks on the side surfaces, and therefore do not separate the original irradiation and LBE embrittlement effects solely.

Figure 8.2.11 shows the results of tensile tests performed in LBE of some samples from the TS-specimens of LiSoR-2 and LiSoR-4 tested in oxygen saturated LBE. For comparison, the result of one LiSoR-2 sample tested in Ar is also included. The embrittlement effects of LBE are clearly demonstrated by the significant reduction of ductility. For the irradiation effects, the results indicate also a trend that the embrittlement effects are more evident at higher doses.

8.2.5 Proton irradiation of pre-oxidised HT9 in the presence of LBE at the LANSCE WNR facility (Los Alamos)

Lillard, *et al*. [Lillard, 2004] investigated pre-oxidised HT9 samples with an oxide scale in the order of 3 μm thickness with impedance spectroscopy while immersed in LBE at 200°C and irradiated with protons in the LANSCE WNR facility.

The energy of the particle beam was 800 MeV and the current of the protons was approximately 63 nA. The impedance spectroscopy was performed before irradiation, during (30 min.) and after irradiation. The results achieved on HT9 pre-oxidised samples during different stages of the experiment diverge among each other and a conclusion concerning the corrosion rate cannot be given definitely. Further experiments are needed to understand fully the process and it has to be critically proven if

Figure 8.2.10. Tensile results of some LiSoR-3 and LiSoR-5 samples performed in Ar

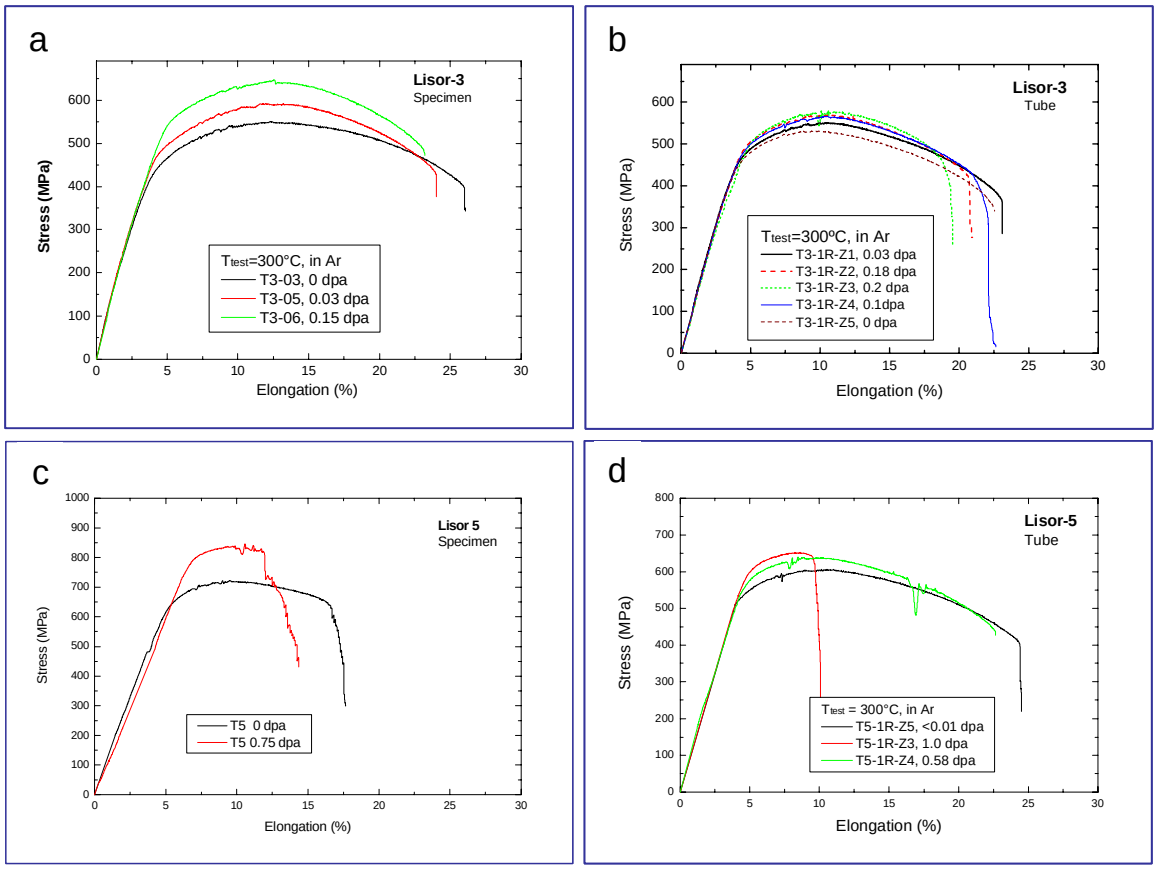

Figure 8.2.11. Tensile results of the some samples from the TS-specimens of LiSoR-2 and -4 tested at 300°C in oxygen saturated LBE; the numbers indicate the irradiation doses

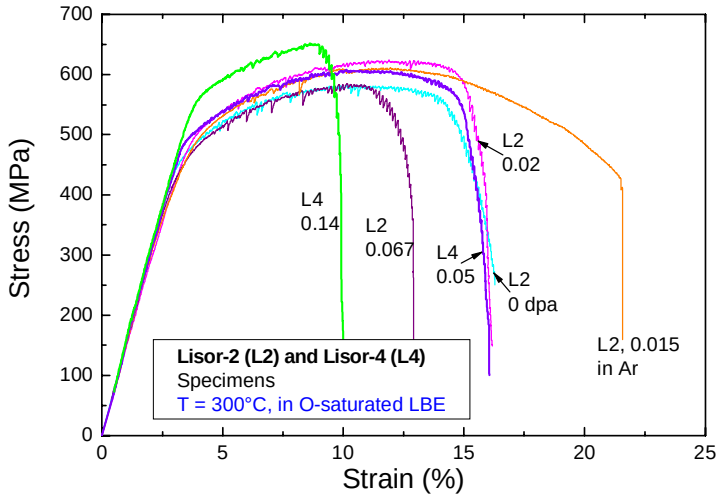

impedance spectroscopy is an appropriate method to assess the corrosion rate in real time during irradiation. It is well-known that beside gamma-ray, X-ray, electron and neutron irradiation [Noda, 1995], [Tanifuji, 1998], [Shikama, 1998], [Vila, 2000] as well proton irradiations of insulating oxides [Sato, 2004], [Hunn, 1995] results in transient radiation induced conductivity (RIC) by promoting electrons from the valence band to the conduction band which can also be the reason of the sharp fall in impedance upon turning the beam on. The RIC effect is up to now mostly observed on ceramic materials like Al_2O_3 and MgO but in [Howlader, 1999] the increase of the electrical conductivity proportional to the irradiation flux was observed on Zircaloy oxides. This might happen as well on oxidised steel surfaces which would adulterate the results of the impedance spectroscopy measured during irradiation.

8.3 Irradiation with neutrons in BR2 (SCK•CEN)

The samples were irradiated in BR-2 reactor in Mol and experimental details and the results of these experiments are taken from the paper of [Sapundjiev, 2005]. The irradiation was done in MISTRAL (Multipurpose Irradiation System for Testing of Reactor ALloys) in-pile sections (MIPS).

8.3.1 Material

The materials tested were austenitic steel AISI 316L and the ferritic-martenisitic steels T91, HT9 and EM10. The chemical compositions of the materials are given in Table 8.3.1.

Table 8.3.1. Chemical composition (wt.%) of AISI 316L, T91, EM10, and HT9 materials tested in liquid Pb-Bi eutectic

MATERIAL	Cr	Ni	Mo	Mn	V	Nb	S	Si	N	C	P	W
AISI 316L (1.4935)	16	10.1	2.1	1.58	–	–	0.016	0.51	–	0.022	0.029	–
T91 (1.4903)	8.3	0.13	0.95	0.4	0.2	0.08		0.4	0.02	0.11	–	<0.01
EM10	8.97	0.07	1.06	0.49	0.013	<0.002	<0.003	0.46	0.014	0.099	0.013	0.01
HT9	11.68	0.66	1.06	0.63	0.29	0.03	<0.003	0.45		0.204	0.020	0.47

The materials were received in the following conditions:

- AISI 316 L: was supplied by SIDERO STAAL, Belgium, n.v., heat number 744060 in the shape of bars with diameter 6 mm and length 500 mm from which the specimens were manufactured. The material is solution annealed with some cold work.
- T91: supplied by UGINE, France, heat 36224 normalised at 1040°C for 60 min. and tempered at 760°C for 60 min.
- EM10: supplied by CEA France, normalised at 990°C for 50 min., tempered at 750°C for 60 min.
- HT9: normalised at 1050°C for 30 min., tempered at 700°C for 2 h.

The samples used were sub-size tensile samples with a length of 27 mm, gage length of 12 mm and diameter of 2.4 mm. The irradiation temperature was about 200°C [Jacquet, 2003]. The fast neutron flux and fluence (E > 1 MeV) were obtained by multiplying the experimental equivalent fission flux and fluence by 0.87, i.e. the average ratio of the calculated fast flux to the equivalent fission flux [Willekens, 2004]. The calculated doses are given in Table 8.3.2.

Table 8.3.2. Irradiation doses and specimen designations of AISI 316L, T91, EM10 and HT9

Material	Dose/dpa	Material	Dose/dpa	Material	Dose/dpa	Material	Dose/dpa
T91	1.14	**AISI 316L**	1.46	**EM10**	2.93	**HT9**	2.53
T91	1.15	**AISI 316L**	1.46	**EM10**	4.36	**HT9**	4.36
T91	1.15	**AISI 316L**	1.57				
T91	1.58	**AISI 316L**	1.72				
T91	1.70						
T91	2.93						
T91	4.36						

8.3.2 Tensile tests

Slow strain rate (SSR) tests were performed in an autoclave in conjunction with a gas conditioning system. All tests in LBE were performed at a strain rate of 5×10^{-6} s^{-1} and a temperature of 200°C. After a sample was broken, it was removed from the autoclave and cleaned in hot tempering oil at 160-180°C for about 5 min.

8.3.3 LBE conditioning

Lead bismuth eutectic alloy (44.8% Pb, 55.2% Bi) was supplied by Hetzel Metalle GmbH, Germany, with reported purity: Pb 99.985% minimum and Bi 99.99% minimum.

Two different oxygen conditions of LBE were investigated. Under oxygen free conditions, the liquid metal was constantly purged with 5% H_2 in Ar gas mixture during the experiment.

The pre-conditioning in both cases (oxygen "free" and oxygen controlled atmosphere) was achieved by bubbling of 5% H_2 in Ar gas mixture or H_2/H_2O mixture respectively into the liquid LBE for approximately 4 hours.

8.3.4 Effect of irradiation and liquid Pb-Bi eutectic on AISI 316L irradiated to 1.7 dpa

The tensile curves from the SSR tests are plotted on Figure 8.3.1. In the same figure the SSRT curve of non-irradiated AISI 316L specimen is given tested under the same conditions for comparison [Sapundjiev, 2004].

Irradiation of AISI 316L resulted in significant hardening and plastic instability after the yield point. The uniform elongation is nearly zero. The stress-strain curves are the same after irradiation up to 1.72 dpa. Their shape does not depend much on the irradiation dose. Irradiation hardening resulted in an increase of the yield (σ_{02}) and tensile (σ_{UTS}) strengths of about 27% and 23%. It seems that the presence of liquid metal had a positive effect on these properties in that σ_{02} and σ_{UTS} decreased with about 3% and 1.5% respectively when tested in LBE which is in the experimental error. Further experiments are needed to clarify if the effect is real.

Regarding the strain to failure, irradiation resulted in irradiation embrittlement and reduction of total elongation of about 27%. When tested in liquid metal the total elongation increased (irrespective to the irradiation dose) by 11-15%, whereas the reduction in area decreased by about 2-11% at different irradiation doses.

Figure 8.3.1. Strain stress curves of A316 L material tested in liquid Pb-Bi at 200°C and strain rate 5.10^{-6} s^{-1}

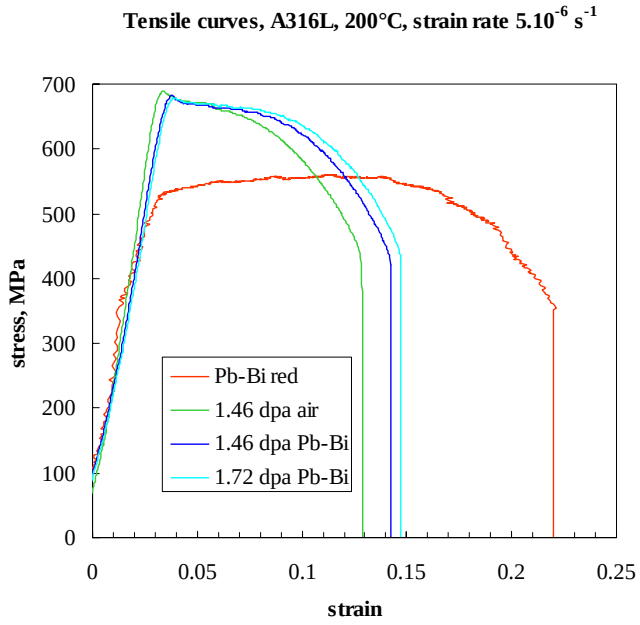

The mechanical parameters of AISI 316L were obtained after the analyses of the stress-strain curves and are presented in Table 8.3.3.

Table 8.3.3. Results of the SSRT tests in liquid Pb-Bi on A 316 L material irradiated to different doses at 200°C and strain rate 5.10^{-6} s^{-1}

Dose/dpa	Environment	$\sigma_{0.2}$, MPa	ε_{tot}, %	ε_{plast}, %	ε_{unif}, %	σ_{UTS}, MPa	$\sigma_{fracture}$, MPa	RA, %
0	Pb-Bi	540.17	24	21	8	559.80	347.96	77±5
1.46	Air (reference)	683.80	13	11	3	689.14	379.44	63±5
1.46	Pb-Bi	670.72	14	12	0	682.38	421.83	56±5
1.57	Pb-Bi+ dissolved oxygen	668.71	15	13	0	685.05	411.96	62±5
1.72	Pb-Bi	663.52	15	13	5	678.94	427.94	59±5

8.3.5 Effect of irradiation and liquid Pb-Bi eutectic on T91 irradiated up to 4.36 dpa

The stress/strain curves of T91 specimens irradiated up to 1.7 dpa and tested in air and in liquid lead-bismuth eutectic are plotted in Figure 8.3.2. The tensile curve of the non-irradiated sample is also provided for comparison, tested in liquid Pb-Bi under the same conditions.

The stress-strain curves of T91 material irradiated to 2.93 and 4.36 dpa are plotted in Figure 8.3.3. In air the material undergoes significant hardening after irradiation and the yield strength approaches about 850 MPa. The irradiation results in reduction of the strain to failure as well. However, the material still deforms plastically although the ultimate and the yield strengths are almost equal. At these doses, the total elongation depends very little on the irradiation dose and tends to saturation.

Figure 8.3.2. Strain stress curves of T91 tested in liquid Pb-Bi at 200°C and strain rate 5.10^{-6} s^{-1}

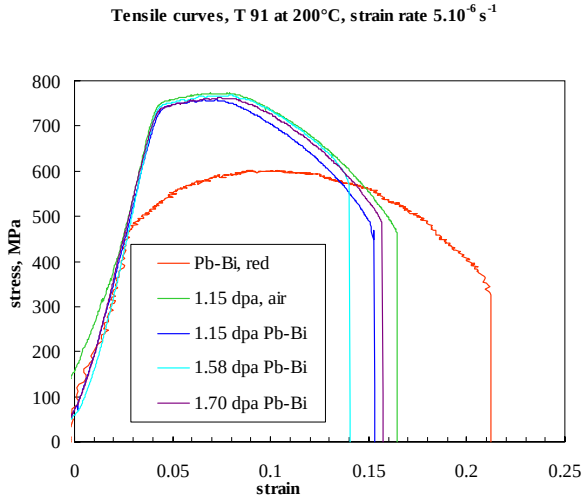

Figure 8.3.3. Tensile curves of irradiated and un-irradiated T91 material tested in liquid Pb-Bi at 200°C at strain rate 5.10^{-6} s^{-1} in Pb-Bi and 3.10^{-4} s^{-1} in air

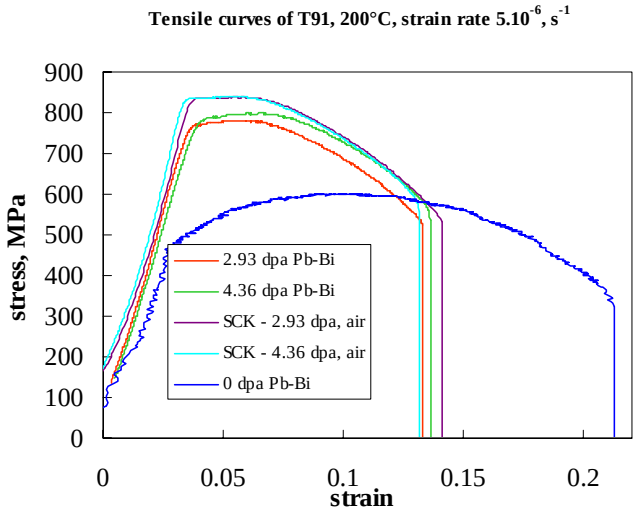

The results of the SSRT tests performed at 200°C on the T91 samples irradiated up to 4.36 dpa are given in Table 8.3.4. The reference tests in air were performed on samples irradiated to 1.15 dpa, 2.93 and 4.36 dpa. The yield and the ultimate tensile strengths approach constant value at doses >2.93 dpa and tend to be invariant of the irradiation dose both in air and in liquid metal. In liquid metal these parameters are always smaller by about 9% and 7% respectively.

8.3.6 Effect of irradiation and liquid Pb-Bi eutectic on EM10 irradiated up to 4.36 dpa

The stress-strain curves of EM10 material tested in air and in liquid lead-bismuth eutectic after irradiation to 4.36 dpa are plotted on Figure 8.3.4. The material has very similar irradiation behaviour to T91. The latter however show higher irradiation hardening (65% increase in σ_{02} and 35% increase in σ_{UTS}) compared to 60% and 25% for EM10 material.

Table 8.3.4. Results of the SSRT tests in liquid Pb-Bi on T91 material irradiated to different doses at 200°C and strain rate 5.10^{-6} s^{-1}

Dose/dpa	Environment	$\sigma_{0.2}$, MPa	ε_{tot}, %	ε_{plast}, %	ε_{unif}, %	σ_{UTS}, MPa	$\sigma_{fracture}$, MPa	RA, %
0	Pb-Bi	482.31	21	19	6	601.23	324.96	77±6
1.14	Pb-Bi + dissolved oxygen	710.75	16	14	3	734.25	424.90	68±5
1.15	Air reference	750.71	16	14	3	772.77	462.66	68±5
1.15	Pb-Bi	731.00	15	13	3	758.31	465.48	61±5
1.58	Pb-Bi	735.40	14	11	4	768.25	531.01	42±3
1.7	Pb-Bi	731.80	16	13	3	763.50	481.66	63±5
2.93	Air	835.00	0.14	0.12	0.02	838.58	531.41	79
4.36	Air	835.28	0.13	0.11	0.03	836.39	554.34	65
2.93	Pb-Bi	756.90	0.13	0.11	0.02	781.93	522.62	64±9
4.36	Pb-Bi	763.90	0.13	0.11	0.03	799.77	536.33	57±9

Figure 8.3.4. Strain stress curves of EM10 material tested in liquid Pb-Bi at 200°C and strain rate 5.10^{-6} s^{-1} in Pb-Bi and 3.10^{-4} s^{-1} in air

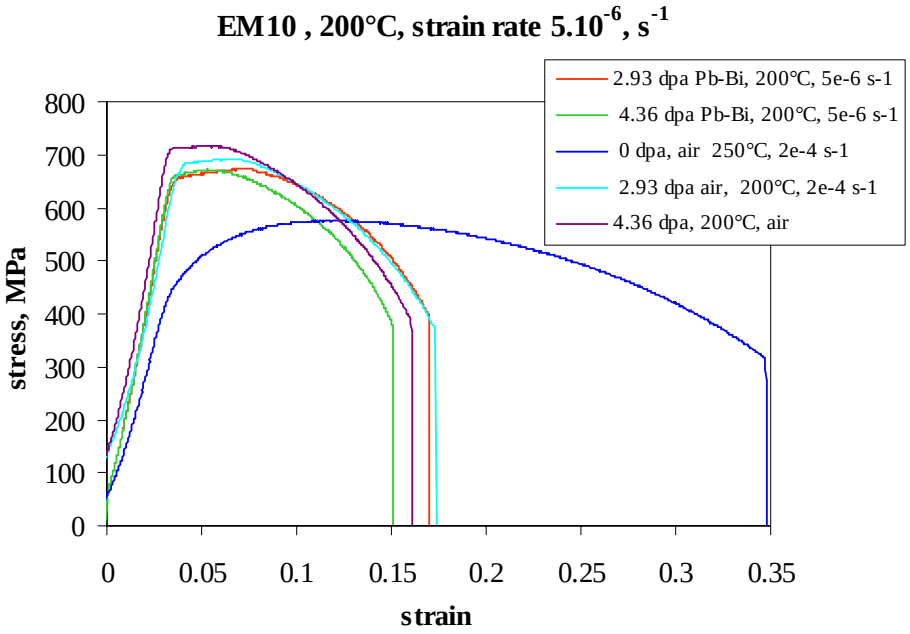

Nevertheless EM10 material still undergoes uniform deformation after irradiation up to 4.36 dpa in air and in LBE. In the latter environment, the total elongation is smaller than in air, but the differences are too small to be assigned to any liquid metal embrittlement. Even at doses as high as 4.36 dpa, the EM10 material deforms plastically and fractures in a ductile manner. The irradiation induced variations decrease with the dose increase and probably will saturate at higher doses. The environmental effect of liquid lead bismuth is very small if it exists at all. The yield and the tensile strengths are slightly smaller in liquid metal than when tested in air.

The results from the SSRT tests on this material irradiated to 2.93 and 4.36 dpa are given in Table 8.3.5 together with the reference tests at the same doses in air as well as the result from the test on non-irradiated material (at 250°C).

Table 8.3.5. Results from the SSRT tests in liquid Pb-Bi on EM10 material irradiated to different doses at 200°C and strain rate 5.10^{-6} s^{-1} when tested in Pb-Bi and 3.10^{-4} s^{-1} for the tests in air

Dose/dpa	Environment	$\sigma_{0.2}$, MPa	ε_{tot}, %	ε_{plast}, %	ε_{unif}, %	σ_{UTS}, MPa	$\sigma_{fracture}$, MPa	RA, %
0*	Air	440.99	35	33	8	576.20	272.82	79-80
2.93	Air	673.39	17	15	2	692.77	357.30	59
4.36	Air	708.27	16	14	2	717.58	368.10	76
2.93	Pb-Bi	643.56	17	15	4	674.25	390.99	74±8
4.36	Pb-Bi	659.54	15	13	2	672.52	378.34	70±9

* At 250°C.

8.3.7 Effect of irradiation and liquid Pb-Bi eutectic on HT9 irradiated up to 4.36 dpa

The stress-strain curves of HT9 material tested in air and in liquid lead-bismuth eutectic after irradiation to 2.53 and 4.36 dpa are plotted on Figure 8.3.5. Irradiation of this material results in hardening and plastic instability reducing mainly the plastic deformation and breaking with almost no necking. The reduction in area when tested in air is about 33 to 34% at 2.53 and 4.36 dpa respectively. In Pb-Bi the reduction in area is slightly higher (38 and 45% at 2.53 and 4.36 dpa).

Figure 8.3.5. Strain stress curves of HT9 material tested in liquid Pb-Bi at 200°C and strain rate 5.10^{-6} s^{-1} in Pb-Bi and 3.10^{-4} s^{-1} in air

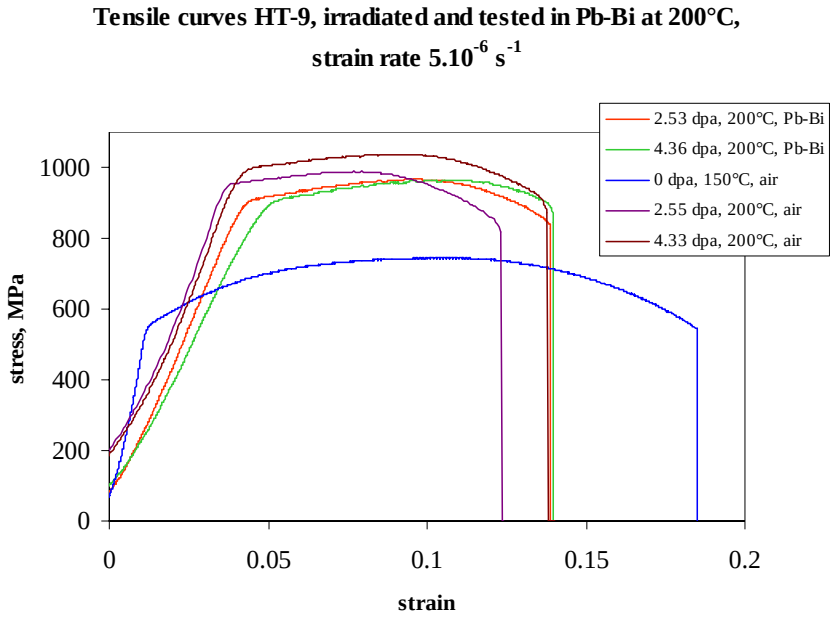

The results of the mechanical tests in air and in liquid metal for HT9 material are summarised in Table 8.3.8. The reference test on non-irradiated material was performed in air and at slightly lower temperature (150°C).

Table 8.3.6. Results of the SSRT tests in liquid Pb-Bi on HT9 material irradiated to different doses at 200°C and strain rate 5.10^{-6} s^{-1} when tested in Pb-Bi and 3.10^{-4} s^{-1} for the tests in air

Dose/dpa	Environment	$\sigma_{0.2}$, MPa	ε_{tot}, %	ε_{plast}, %	ε_{unif}, %	σ_{UTS}, MPa	$\sigma_{fracture}$, MPa	RA, %
0*	Air	559.62	18	17	9	744.73	544.90	61
2.53	Air	960.30	12	9	4	988.86	819.79	33
4.36	Air	977.91	14	10	5	1037.52	871.23	34
2.53	Pb-Bi	896.00	14	10	5	967.01	826.79	38±11
4.36	Pb-Bi	841.00	14	10	6	965.38	846.74	45±10

* At 150°C.

The yield and the tensile strength of HT9 increased by about 72% and 20% at 2.53 dpa and 75% and 25% at 4.36 dpa respectively. Both properties tend to saturation with the irradiation dose as with the previous materials. The effect of the liquid metal is somehow positive on the strength properties. When tested in Pb-Bi the yield and the tensile strength decreased with 7% and 2% at 2.53 dpa and with 14% and 7% at 4.36 dpa respectively compared to the same conditions in air. The SEM inspection of the fracture face of the different samples revealed no difference of their fractures independent on the testing environment.

8.4 Irradiation with proton and neutron spectrum in SINQ targets at PSI

In the SINQ target irradiation programme (STIP) many samples were irradiated or are being irradiated in presence of LBE and pure Pb as well.

In STIP-II [Dai, 2005] which was performed in 2000 and 2001, about 150 samples of different types such as tensile, bending-fatigue, TEM and stressed capsules from more than 10 kinds of ferritic/ martensitic (FM) and austenitic steels were irradiated to doses up to 19 dpa in the temperature range 100 to 400°C. In particular, some TEM discs were coated with different kinds of materials by using several methods. Part of these samples have been retrieved and being analysed. The preliminary results should be available around in the end of 2006, and detailed investigations should be completed in 2007.

In STIP-IV which is being conducted in the present SINQ target, a number of T91 and SS 316LN samples are being irradiated in contact with LBE and Pb. The irradiation temperature is up to 500°C and the final irradiation dose should be about 20 dpa when the irradiation completed by the end of 2005. The PIE will be performed in 2008.

8.4.1 Mechanical tests on irradiated specimens in LBE

Some FM steel specimens irradiated in STIP-I [Dai, 2001] have been tested in LBE. Figure 8.4.1 shows results from a three-point bending test on pre-cracked T91 samples in Ar and LBE (oxygen saturated) environments [Dai, 2006a]. As illustrated in Figure 8.4.1, LBE embrittlement effect is very clear. For the sample tested in LBE, the crack propagated suddenly through the whole specimen after three loading-unloading cycles and resulted in a brittle fracture. The corresponding fracture toughness value is about 40 MPa√m, which is significantly lower than that of tested in Ar, 105 MPa√m. Systematic tensile and bending tests on sample irradiated in STIP-I and STIP-II will be conducted in 2005 to 2007.

Figure 8.4.1. Load-displacement curves of irradiated T91 specimens tested at 250°C in Ar and LBE (oxygen saturated)

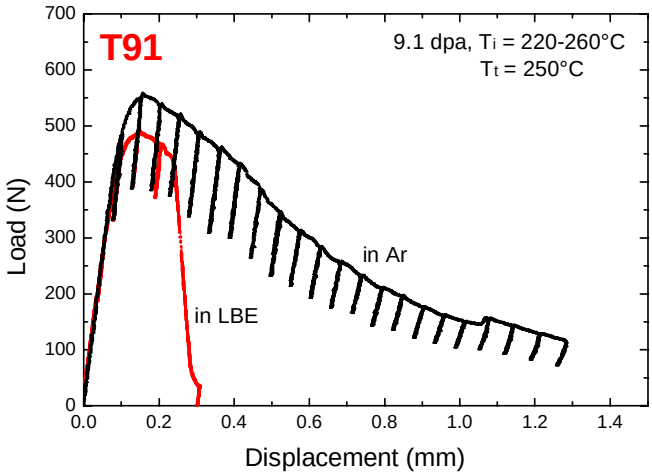

The higher dose may be one reason for the different results achieved on HT9 and were described in the previous section. But the main difference is that the three-point bending tests were performed on "pre-cracked" samples, while the tensile samples irradiated in Mol were smooth samples. SSRT results [Dai, 2006c] on un-irradiated T91 tensile samples indicate that without surface cracks the LME of LBE is hardly to take place. Up to now the results are very limited and further experiments are needed to compare the results achieved on different mechanical testing procedures.

8.5 Future irradiation programmes (DEMETRA programme)

Experimental programme on neutron irradiation/LBE combined effects foreseen in the European project EUROTRANS

In the frame of the DEMETRA domain of the EUROTRANS project, a work package has been foreseen for the study and compilation of data on the irradiation behaviour of reference structural materials in the specific environment of accelerator-driven systems. Two types of reference structural materials were defined: the stainless steel AISI 316L that will be considered for the vessel components and the martensitic steel T91 (9Cr1MoVNb) envisaged for the spallation target structures and core components. In addition, for components in the high temperature regions of the ADS (i.e. core), the use of Fe-Al based coatings is anticipated.

It is well known that irradiation induces specific effects such as defect production (displacement of atoms, dislocation loops, and voids), phase instability (dissolution, precipitation, segregation), changes in chemical composition induced by spallation or transmutation reactions. These important modifications in the material microstructure induce a degradation of mechanical properties, which will affect the lifetime of different components. Besides the consideration on "pure" irradiation, other important contribution to the lifetime of components comes from the presence of flowing LBE alloy. Corrosion mechanisms and embrittlement phenomena can further limit the performances of structural materials.

The experimental approach foreseen within DEMETRA will consist on testing materials with different available experimental tools, like fission reactors including irradiation in LBE, irradiation under mixed proton/neutron spectrum, helium and implantation tests. The experimental activities aim

at studying the combined effects, like in the case of irradiations in presence of LBE in a neutron field, but also to determine and separate each damaging contribution to enhance comprehension of irradiation phenomena.

To investigate the combined effects induced by the irradiation in presence of liquid LBE alloy and to evaluate the contribution of corrosion mechanisms and irradiation damage on the degradation of mechanical properties of T91 steel and selected coatings two irradiation experiments are foreseen. The irradiations will be conducted in the two irradiation facilities BR2 and HFR respectively. BR2 and HFR are two mixed spectrum fission reactors operated by SCK•CEN, Mol, Belgium and NRG, Petten, Netherlands, respectively.

In Table 8.5.1 the test matrix foreseen for the two reactors are reported. This table shows that the irradiation experiments will be performed on the T91 steel in a temperature range of 300-500°C and in a dpa range of 2-5. In addition, in the high temperature range (450 and 500°C), samples of coated T91 steel will be irradiated.

The preparation of the irradiation rig and the licensing of the experiments are started at the time being of preparing this handbook. The set of results of the post-irradiation experiments will be available by the beginning of 2009.

Table 8.5.1. Test matrix of the HFR and BR2 experiments

Reactor	**HFR – NRG**	**BR-2 – SCK•CEN**	
Irradiation temperature	350°C and 500°C	300°C	450°C
Damage	2 dpa	2 dpa	5 dpa
Material	T91/coating	T91	T91/coating
Duration	2 dpa, 1 y or 2 dpa, 0.7 y	1.5 y	2 y
Environment	LBE	LBE and H_2O	LBE and gas
O_2 content	<10E-6	<10E-6 & saturated	<10E-6 &saturated
Samples	2*8 Tensile 2*8 Tensile notched 2*8 KLST 2*8 pre-stressed 2*8 corrosion/coating	24 SSRT 24 control H_2O 36 water 24 CT 10.3 mm 24 CT water plates, corrosion coating	2 CT 2 CT weld 36 tubes
PIE performed in LBE	With oxygen-controlled atmosphere	Controlled gas phase and LBE	Controlled gas phase and LBE
	Po measurements		Po analyses

REFERENCES

Dai, Y., G.S. Bauer (2001), "Status of the first SINQ irradiation experiment, STIP-I", *Journal of Nuclear Materials*, Vol. 296, pp. 43-53.

Dai, Y., H. Glasbrenner, V. Boutellier, R. Bruetsch, X. Jia, F. Groeschel (2004), "Preliminary Results of Post-irradiation Examinations on LiSoR-2 Test Section", *Journal of Nuclear Materials*, Vol. 335, pp. 232-238.

Dai, Y., X. Jia, R. Thermer, D. Hamaguchi, K. Geismann, E. Lehmann, H.P. Linder, M. James, F. Groeschel, W. Wagner, G.S. Bauer (2005), "The Second SINQ Target Irradiation Program, STIP-II", *Journal of Nuclear Materials*, Vol. 343, pp. 33-44.

Dai, Y., *et al*. (2006a), "An Assessment of the Window Lifetime of MEGAPIE Target Liquid Metal Container", *Journal of Nuclear Materials*, Vol. 356, pp. 308-320.

Dai, Y., B. Oliver (2006b), "A Comparison Between Calculated and Measured He and H Contents of STIP Samples", *7th International Workshop on Spallation Materials Technology*, 29 May-3 June 2005, Thun, Switzerland.

Dai, Y., B. Long, X. Jia, H. Glasbrenner, K. Samec, F. Groeschel (2006c), "Tensile Tests and TEM Investigations on LiSoR-2 to -4", *Journal of Nuclear Materials*, Vol. 356, pp.256-263.

Fazio, C., A. Alamo, A. Almazouzi, D. Gomez-Briceno, F. Groeschel, F. Roelofs, P. Turroni, J.U. Knebel (2005), "Assessment of Reference Structural Materials, Heavy Liquid Metal Technology and Thermal-hydraulics for European Waste Transmutation ADS", *Proceedings of GLOBAL 2005*, Tsukuba, Japan, 9-13 Oct..

Glasbrenner, H., Y. Dai, F. Groeschel (2005a), "LiSoR Irradiation Experiments and Preliminary Post-irradiation Examinations", *Journal of Nuclear Materials*, Vol. 343, pp. 267-274.

Glasbrenner, H., Y. Dai, F. Groeschel (2005b), "LiSoR Experiment: Overview and Relevant Results for MEGAPIE", *TRM-MEGAPIE Meeting*, Mol, Belgium.

Glasbrenner, H., R. Bruetsch, Y. Dai, F. Groeschel, M. Martin (2006), "Inspection of Samples Irradiated in LiSoR-3", *IWSMT-7*, Thun, Switzerland, 2005, forthcoming in *Journal of Nuclear Materials*.

Howlader, M.M.R., C. Kinnoshita, K. Shiiyama, M. Kutsuwade, M. Inagaki (1999), "*In Situ* Measurement of Electrical Conductivity of Zircaloy Oxides and Their Formation Mechanism Under Electron Irradiation", *Journal of Nuclear Materials*, Vol. 265, pp. 100-107.

Hunn, J.D., R.E. Stoller, S.J. Zinkle (1995), "*In-situ* Measurement of Radiation-induced Conductivity of Thin Film Ceramics", *Journal of Nuclear Materials*, Vol. 219, pp. 169-175.

JNM (2004), Proceedings of the 3rd International Workshop "Materials for Hybrid Reactors and Related Rechnologies", *Journal of Nuclear Materials*, Vol. 335, No. 2.

Jung, P. (2002), "Radiation Effects in Structural mMterials of Spallation Targets", *Journal of Nuclear Materials*, Vol. 301, pp. 15-22.

Kirchner T., *et al*. (2003), "LiSoR, a Liquid Metal Loop for Material Investigation Under Irradiation", *Journal of Nuclear Materials*, Vol. 318, pp. 70-83.

Jacquet P. (2003), *Irradiation Achieved in BR2 During Cycle 05/2002 from 26 November 2002 to 17 December 2002*, SCK•CEN Internal Memo, MI.57/D089010/02/PJ, 10 February 2003.

Lillard, R.S., M. Paciotti, V. Tcharnotskaia (2004), "The Influence of Proton Irradiation on the Corrosion of HT-9 During Immersion in Lead Bismuth Eutectic", *Journal of Nuclear Materials*, Vol. 335, pp. 487-492.

Samec, K. (2005), *Temperature Calculations of the LiSoR Experiment*, PSI Technical Report, TM-34-05-02.

Sapundjiev, D., A. Al Mazouzi, S. Van Dyck (2004), *Synergetic Effects Between Neutron Irradiation and LME: PIE Tests in Lead-bismuth Eutectic, Part I: Tests on Non-irradiated Samples*, SCK•CEN Report, R-3847, March 2004.

Sapundjiev, D., E. Lucon, M. Matijasevic, S. Van Dyck, A. Almazouzi (2005), "Mechanical Behaviour of Candidate Steels in LBE After Irradiation in BR2 at 200°C", *Journal of Nuclear Materials*, Vol. 356, pp. 229-236.

Sato, F., T. Tanaka, T. Kagawa, T. Iida (2004), "Impedance Measurements of Thin Film Ceramics Under Ion Beam Irradiation", *Journal of Nuclear Materials*, Vol. 329-333, pp. 1034-1037.

Shikama, T., S.J. Zinkle, K. Shiiyama, L.L. Snead, E.H. Farnum (1998), "Electrical Properties of Ceramic During Reactor Irradiation", *Journal of Nuclear Materials*, Vol. 258-263, pp. 1867-1872.

Tanifuj, T., Y. Katano, T. Nakazawa, K. Noda (1998), "Electrical Conductivity Change in Single Crystal Al_2O_3 and MgO Under Neutron and Gamma-ray Irradiation", *Journal of Nuclear Materials*, Vol. 253, pp. 156-166.

Vila, R., E.R. Hodgson (2000), "In-beam Dielectric Properties of Alumina at Low Frequencies", *Journal of Nuclear Materials*, Vol. 283-287, pp. 903-906.

Willekens, M. (2004), *Neutron Dosimetry – Experiment SPIRE*, Technical Note RF&M/VWi/vwi 32.D049011-205/04-01, 14/01/2004.